UV LASER PHOTOLYSIS OF C_3O_2 AT 193 nm: EMISSION FROM ELECTRONICALLY EXCITED C, CO AND C_2

M. UMEMOTO, H. SHINOHARA and N. NISHI

Institute for Molecular Science, Myodaiji, Okazaki 444 (Japan)

R. SHIMADA

Department of Chemistry, Faculty of Science, Kyushu University, Hakozaki, Higashi-ku, Fukuoka 812 (Japan)

(Received April 21, 1982)

Summary

C_3O_2 was irradiated using an ArF pulsed excimer laser at 193 nm and fluorescence from electronically excited CO and C was observed. The CO($A\ ^1\Pi \rightarrow X\ ^1\Sigma^+$) fourth positive emission at 200 - 250 nm results from the production of a vibrationally excited CO($X\ ^1\Sigma^+$) fragment which is resonantly pumped to the $A\ ^1\Pi(v' = 1, 4, 7)$ state at 193 nm. The C($3\ ^1P^0 \rightarrow 2\ ^1S$) emission at 248 nm is attributed to a two-step process; two-photon generation of the C($2\ ^1D$) state and consequent resonant excitation of the carbon atom to the $3\ ^1P^0$ state. The C_2($d\ ^3\Pi_g \rightarrow a\ ^3\Pi_u$) Swan high pressure band was also observed and was attributed to the collision-induced reaction between C and C_2O.

1. Introduction

The recent development of a new light sou. ', the high power pulsed excimer laser, has made possible the elucidation of hitherto unresolved questions concerning dissociation processes occurring from highly excited electronic states of molecules in the gas phase. This laser delivers a high intensity photon flux and is therefore suitable for multiphoton excitation. Significant concentrations of electronically excited photofragments can be generated through dissociation of the highly excited states produced by multiphoton excitation. A large number of experiments based upon this property of the excimer laser have been performed in recent years [1].

Carbon suboxide (C_3O_2) is a constituent of the atmosphere of Venus [2] and is a possible origin of the reddish colour of the martian surface [3]. The photochemistry of C_3O_2 with a broad-band light source has been investigated extensively. The vapour phase photochemistry of C_3O_2 has recently been reviewed by Filseth [4]. The absence of fluorescence on irradiation

0047-2670/82/0000-0000/$02.75

with a mercury lamp would suggest that it is efficiently decomposed in the UV region [5]. Two primary processes have been proposed for C_3O_2 photolysis. These are (1) breaking of a C—C bond to yield the C_2O radical and CO and (2) breaking of two C—C bonds to yield a carbon atom and two CO molecules. The photolysis of C_3O_2 in the presence of ethylene results in the production of allene [6]. It is believed that C_2O is the reactive intermediate in this reaction. The vacuum UV flash photolysis of C_3O_2 has been investigated by Braun *et al.* [7] who observed absorption from three carbon atom states, C(2 ^{3}P), C(2 ^{1}S) and C(2 ^{1}D).

In this paper we report the multiphoton dissociation of C_3O_2 excited at 193 nm which results in the production of electronically excited atoms, radicals and molecules.

2. Experimental details

The apparatus used in this work was essentially the same as that described in a previous paper [8]. The excitation source was a Lumonics TE-861 rare gas halide excimer laser which was operated with a static gas mixture. The ArF laser delivers pulses of duration 10 ns and spectral bandwidth about 170 cm^{-1} full width at half-maximum at 193 nm. The power per pulse is about 100 mJ. The laser beam was focused approximately at the centre of a spherical cell 16 cm in diameter with side-arms equipped with Suprasil windows set at the Brewster angle. In order to reduce the effects of scattered light a Wood's horn was located opposite the observation window. The photon flux at the focusing point was estimated to be about 10^{25} photons cm^{-2} s^{-1} at 193 nm. In some experiments C_3O_2 was irradiated using a 248 nm KrF laser with an output power of 150 mJ per pulse. The fluorescence was observed at right angles to the laser beam using in the visible region a Spex 1704 spectrometer equipped with an RCA C31034 photomultiplier tube (PMT) and in the UV region a Jobin–Yvon HRD-2 spectrometer with a Hamamatsu R-955 PMT. The signal from the PMT was gated and averaged using a Brookdeal 9415 linear gate and was then displayed on a strip chart recorder.

While the fluorescence spectrum was being recorded, a continuous flow of sample gas was passed through the cell in order to eliminate effects due to photolysis products. The flow rate was controlled using a needle valve and an MKS Baratron type 221 capacitance manometer. Transient profiles of the fluorescence were obtained using an HP1744 storage oscilloscope. The photoproducts were analysed using a JEOL JMS D300 high resolution mass spectrometer.

C_3O_2 was prepared by the dehydration of malonic acid with P_2O_5 at 120 - 140 °C [9]. The major impurities were acetic acid and CO_2. The acetic acid was removed by distillation from an ice-water bath to a liquid nitrogen trap. The CO_2 was distilled off under reduced pressure from an ethanol freezing bath to a liquid nitrogen trap. The purity was checked by both IR and mass spectroscopy.

3. Results and discussion

3.1. Mass analysis of photoproducts

C_3O_2 in a static cell at a pressure of 1.0 Torr was irradiated with 3000 shots of the ArF laser pulse. Immediately after the photolysis the photoproducts were analysed using the mass spectrometer. The analysis shows that the parent molecule was completely decomposed. CO was the only gaseous reaction product detected. It was also observed that carbonaceous solids were deposited on the surface of the photolysis cell. It is probable that reactive species such as C, C_2 and C_2O, generated by the photolysis, are trapped on the cell surface and polymerize. Such species also react with C_3O_2 molecules to yield carbon-rich polymers.

3.2. Emission from electronically excited fragments

Figure 1 shows the emission spectrum observed when 0.70 Torr of C_3O_2 in a flow condition was irradiated by the laser at 193 nm. Several emission bands are observed in the 200 - 250 nm region together with a sharp atomic carbon line at 248 nm. The interval between the band peaks is 1500 - 1800 cm^{-1} which is characteristic of the stretching vibration of CO. As mentioned earlier, CO is a product of C_3O_2 photolysis and may possibly be excited by multiphoton absorption with subsequent fluorescence in this region. Upon irradiation of 1.0 Torr of CO gas itself, however, these bands could not be observed. We can therefore conclude that this emission results not from the excitation of CO produced by the photofragmentation but from the direct dissociation of C_3O_2. This conclusion is confirmed by the cell experiments, the results of which are shown in Fig. 2. It can be seen that the intensity of the CO fluorescence decreases gradually as the number of shots increases despite the accumulation of ground state CO. It should also be emphasized that the emission spectrum was recorded under flow conditions in which the contribution to the emission from the photolytic products was negligible.

Further information regarding this system was furnished by emission lifetime measurements performed at each of the band peaks and tails. The rise time of the signal followed the laser pulse, while the emission decayed with a lifetime of 20 ns or less. Three band systems are known to exist in this spectral region: the fourth positive system ($A\ ^1\Pi - X\ ^1\Sigma^+$), the 3A bands ($c\ ^3\Pi - a\ ^3\Pi$) and the Cameron bands ($a\ ^3\Pi - X\ ^1\Sigma^+$). The 3A bands can safely be excluded because of the inconsistency between the observed band locations and data reported in the literature [10]. The Cameron bands can be excluded since they result from a spin-forbidden transition which has a lifetime of 7.5 - 9.5 ms [11]. Hence we assign this system to the fourth positive system. The lifetime of the fourth positive band was measured by Hesser [12] as about 10 ns and by Chervenak and Anderson [13] as about 16 ns in good agreement with our experiment.

Figure 3 shows the relative fluorescence intensities as a function of the relative laser intensity. The CO fluorescence intensity depends on the 2.3

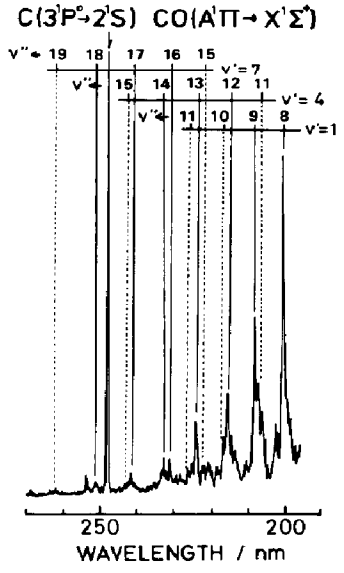

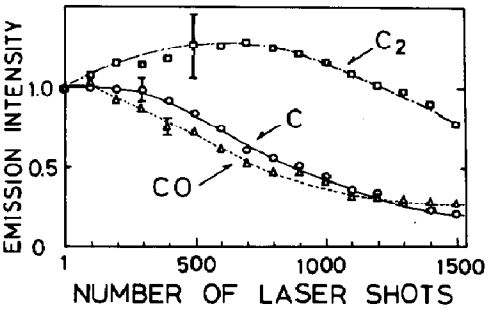

Fig. 1. C(3 $^1P^0$ → 2 ^1S) and CO(A $^1\Pi$ → X $^1\Sigma^+$) fluorescence spectra obtained on the photolysis of 0.70 Torr of C_3O_2 at 193 nm.

Fig. 2. Relative intensity changes in C, C_2 and CO fluorescence occurring in the photolysis of 0.70 Torr of C_3O_2 in a static cell as a function of the number of irradiating pulses. The initial intensity is normalized to unity.

power of the incident laser intensity. At higher laser intensities, however, a saturation effect was observed. Therefore at least three photons are required for the CO(A $^1\Pi$) formation.

The emission originates from particular vibrational levels ($v' = 1, 4, 7$) of the A $^1\Pi$ state. A resonant pumping process is assumed to contribute to this three-photon pathway. Figure 4 shows the ArF laser spectrum and the calculated intensity distributions for some of the CO(A $^1\Pi$–X $^1\Sigma^+$) rovibronic transitions. The intensity distribution is expressed as a product of the line strength S_J and the Boltzmann factor [14]:

$$I_{abs} \propto S_J \exp\left\{-\frac{B''J''(J''+1)hc}{kT}\right\}$$

In this expression the frequency factor and a constant factor depending on the change in dipole moment and the total number of molecules in the initial vibrational level are disregarded. For a given rotation–vibration band at a given temperature the frequency factor is nearly constant, but for the intensity distribution under discussion here a small variation of this factor must be taken into account. According to the Hönl–London formula, the line strength for $\Delta\Lambda = +1$ in the Q branch is given by

$$S_J^Q = \frac{(J''+1+\Lambda'')(J''-\Lambda'')(2J''+1)}{4J''(J''+1)}$$

The intensity distribution in the Q branch is calculated because in the

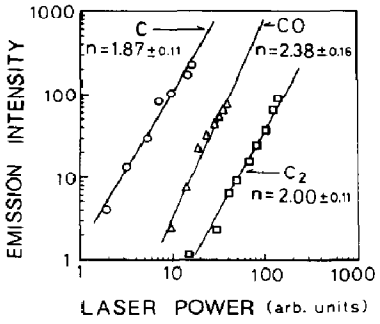

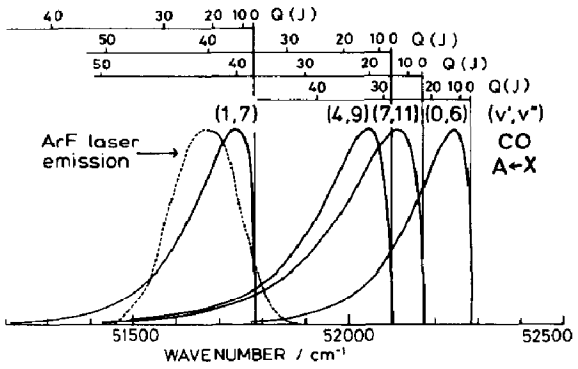

Fig. 3. Fluorescence intensity I as a function of the laser power E. The data are the least-squares fit to $I \propto E^n$. The standard deviations are $\pm\sigma$.

Fig. 4. ArF laser emission spectrum and calculated absorption intensity distributions for the A $^1\Pi$ (v', J) ← X $^1\Sigma^+$ (v'', J) transitions. The rotational temperature is assumed to be 1000 K and each absorption intensity is normalized to the same peak intensity.

$^1\Pi$–$^1\Sigma$ transition the lines of the Q branch have approximately twice the intensity of the corresponding lines of the P or the R branch. Since C_3O_2 is expected to have a bent structure even in lower excited states [15], it is reasonable to assume that rotationally excited fragments are produced. A rotational temperature of 1000 K is assumed in the calculation. If the CO photofragment is not excited rotationally (*i.e.* it is in thermal equilibrium at room temperature), resonant pumping from the $v'' = 9$ and $v'' = 11$ levels would fail. All other transitions from $v'' = 6$ - 11 are located out of the energy region shown in Fig. 4. The spectroscopic data used in the calculation were taken from ref. 11.

Taking into account the known thermochemical data [16], we propose that CO(A $^1\Pi$) is formed according to the following mechanism:

$$C_3O_2 \xrightarrow{2h\nu} C(2\,^1D) + 2CO(X\,^1\Sigma^+, \text{rotationally and vibrationally excited}) \quad (I)$$

$$CO(X\,^1\Sigma^+, v'' = 7, 9, 11) \xrightarrow[\text{resonant pumping}]{h\nu} CO(A\,^1\Pi, v' = 1, 4, 7) \quad (II)$$

In process (I) it is energetically possible to excite the two CO molecules to the $v'' = 11$ vibrational level. The rotationally and vibrationally excited CO molecule at levels $v'' = 7$, $v'' = 9$ or $v'' = 11$ then resonantly absorbs a single 193 nm photon and yields the $v' = 1$, $v' = 4$ or $v' = 7$ levels respectively in the A $^1\Pi$ state. The saturation effect at higher laser intensities arises from resonant absorption of a third photon.

In addition to the CO fluorescence, excitation at 193 nm also led to a sharp emission at 247.8 nm as illustrated in Fig. 5. This emission can be unambiguously assigned to the carbon atom 3 $^1P^0 \rightarrow 2\,^1S$ transition. The rise of this fluorescence follows the laser pulse, implying direct formation of an excited carbon atom from a parent molecule. The decay time is equal to or

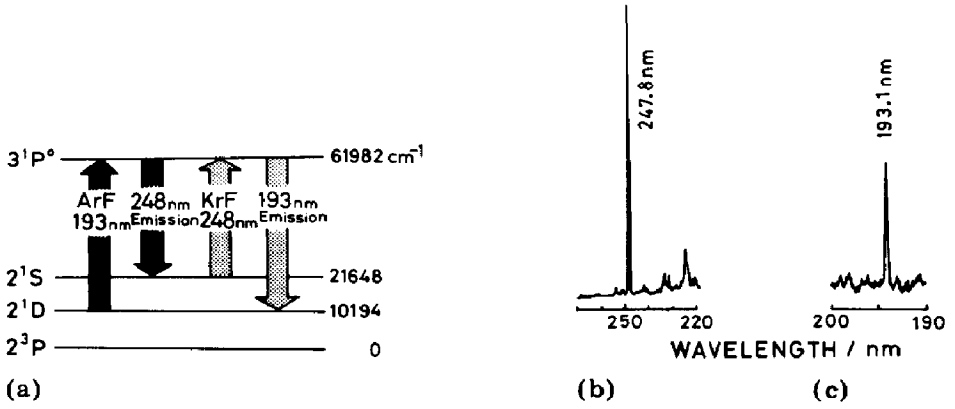

Fig. 5. (a) Energy level diagram of the carbon atom (the arrows show the resonant absorptions and radiative transitions discussed in the text); (b) C(3 $^1P^0$) → C(2 ^1S) emission occurring during ArF laser photolysis of C_3O_2 at 193 nm; (c) C(3 $^1P^0$) → C(2 ^1D) emission occurring during KrF laser photolysis of C_3O_2 at 248 nm.

shorter than the duration of the laser pulse (10 ns or less). An experiment under static cell conditions also supports the direct formation mechanism. The fluorescence intensity decreases monotonically as a function of the number of laser pulses as shown in Fig. 2. Therefore it is concluded that the electronically excited carbon atom is formed by a primary process in the C_3O_2 photolysis.

The pathway of least energy by which the C(3 $^1P^0$) state can be produced from ground state C_3O_2 is

$$C_3O_2 \rightarrow C(3\ ^1P^0) + 2CO(X\ ^1\Sigma^+) \qquad \Delta H = 13.8\ \text{eV} \qquad \text{(III)}$$

Absorption of at least three photons of 193 nm (6.4 eV) light is necessary for this dissociation process to take place. However, the plot in Fig. 3 shows that the fluorescence intensity at 248 nm depends approximately on the square of the laser power. This dependence is explained on the basis of a two-photon dissociation step followed by a resonant absorption at 193 nm. Bokor *et al.* [17] have observed a similar process in the photolysis of CO utilizing an ArF laser. The emission mechanism of the carbon atom is illustrated in Fig. 5. At first, C(2 ^1D) is produced in the two-photon absorption process

$$C_3O_2 \rightarrow C(2\ ^1D) + 2CO(X\ ^1\Sigma^+) \qquad \Delta H = 7.35\ \text{eV} \qquad \text{(IV)}$$

This is followed by resonant absorption in the allowed transition C(3 $^1P^0$) → C(2 ^1D) owing to an accidental coincidence between this transition energy and the excitation laser energy. As this resonant absorption is strongly saturated at higher intensities, we observe an overall quadratic power dependence. It should be noted that the transition C(2 ^1D) → C(2 ^3P) is forbidden and that the C(2 ^1D) state has a lifetime of 53 min. The C(3 $^1P^0$) → C(2 ^1D) transition may produce fluorescence at 193 nm, but it is not possible to separate this emission from the scattered excitation light.

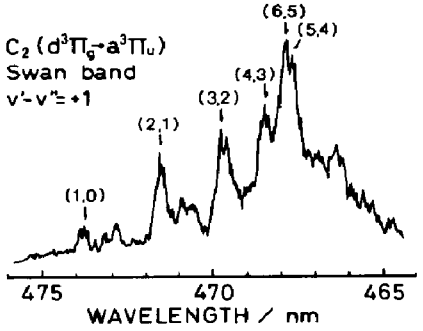

Fig. 6. $C_2(d\ ^3\Pi_g \rightarrow a\ ^3\Pi_u)$ Swan band $v' - v'' = +1$ sequence emission occurring during the photolysis of C_3O_2 (0.50 Torr) at 193 nm.

An accidental coincidence of the laser energy with the transition energy of the carbon atom also occurs in the 248 nm photolysis of C_3O_2. In this case the KrF laser energy and the energy of the allowed $C(3\ ^1P^0) \rightarrow C(2\ ^1S)$ transition are the same. The $C(2\ ^1S) \rightarrow C(2\ ^1D)$ and $C(2\ ^1S) \rightarrow C(2\ ^3P)$ transitions are forbidden and the lifetime of the $C(2\ ^1S)$ state is 2 s. If $C(2\ ^1S)$ is produced during the 248 nm photolysis of C_3O_2, we might expect that $C(3\ ^1P^0)$ would be resonantly created from $C(2\ ^1S)$ by absorption of the KrF laser line. $C(3\ ^1P^0) \rightarrow C(2\ ^1D)$ fluorescence at 193 nm would then be expected. As the spectrum in Fig. 5(c) indicates, we did indeed observe carbon atom emission at 193 nm during photolysis at 248 nm.

Upon irradiation of C_3O_2 by the ArF laser, the $v' - v'' = +1$ sequence of the C_2 ($d\ ^3\Pi_g \rightarrow a\ ^3\Pi_u$) Swan system was identified in the spectral range between 465 and 475 nm. Figure 6 shows the fluorescence spectrum obtained for 0.5 Torr of C_3O_2. The Swan band emission shows the characteristic profile of the so-called "high pressure bands" [10]. Selective population of the $v' = 6$ vibrational level in the $d\ ^3\Pi_g$ state of C_2 is conspicuous. The terminology of the high pressure band is derived from the fact that this emission occurs in condensed discharges through CO at relatively high pressures (10 - 100 Torr). They were initially considered as a separate band system but have now been shown by isotope studies [18] to be a part of the Swan system.

Recently, C_2 high pressure bands have been observed at pressures of about 10 Torr and above in the UV multiphoton photolysis of CO. In the present photolysis of C_3O_2 the high pressure bands were observed even at pressures as low as 0.1 Torr. We consider that the C_2 high pressure bands are formed by the reaction $C + C_2O \rightarrow C_2^* + CO$. Therefore the appearance of the bands at relatively low pressures suggests that the two species C and C_2O are produced efficiently in the photolysis of C_3O_2. The formation mechanism of C_2^* will be discussed in the following section.

3.3. Kinetics of the C_2 Swan band emission

An analysis of the transient profile of the C_2^* fluorescence was carried out in order to investigate the mechanism of production of the C_2 high pressure bands. Figure 7 shows typical rise and decay curves measured at 468 nm (v', v'' = 6, 5) for 1.5 and 5.0 Torr of C_3O_2. The C_2 emission has a much

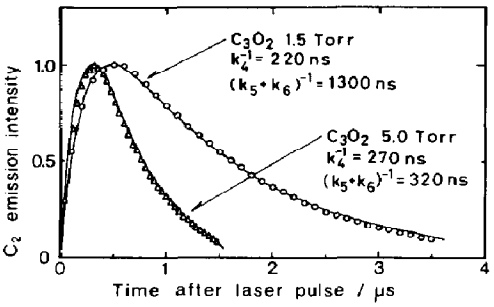

Fig. 7. C_2 Swan fluorescence intensity as a function of time following the photolysis of C_3O_2 at 193 nm: ○, fluorescence data at 1.5 Torr; △, fluorescence data at 5.0 Torr; ———, derived from computer fits using eqn. (10). The fluorescence was monitored at 468 nm (v', v'' = 6, 5).

slower rise time than the duration of the laser pulse (10 ns). Its decay is very long lived compared with the known radiative lifetimes (200 ± 50 ns [19] and 170 ± 20 ns [20]). These facts suggest that C_2^* is not produced by the direct dissociation of C_3O_2 but by a secondary process involving the photolysis products.

We therefore propose the following reaction sequence to explain the observed C_2^* fluorescence characteristics:

$$C_3O_2(X\ ^1\Sigma_g^+) \xrightarrow{h\nu(193\ nm)} C(2\ ^3P) + 2CO(X\ ^1\Sigma^+) \qquad \Delta H = 6.09\ eV \qquad (1)$$

$$C_3O_2(X\ ^1\Sigma_g^+) \xrightarrow{h\nu(193\ nm)} C_2O(a\ ^1\Delta) + CO(X\ ^1\Sigma^+) \qquad \Delta H = 3.31\ eV \qquad (2)$$

$$C(2\ ^3P) + C_2O(a\ ^1\Delta) \xrightarrow{k_3} C_2(d\ ^3\Pi_g) + CO(X\ ^1\Sigma^+) \qquad \Delta H = -0.877\ eV \qquad (3)$$

$$C_2(d\ ^3\Pi_g) \xrightarrow{k_4} C_2(a\ ^3\Pi_u) + h\nu\ (\text{Swan band}) \qquad (4)$$

$$C(2\ ^3P) + M_i \xrightarrow{k_5} \text{product} \qquad (5)$$

$$C_2O(a\ ^1\Delta) + M_i \xrightarrow{k_6} \text{product} \qquad (6)$$

where M_i stands for C_3O_2 or other photoproducts.

In processes (1) and (2) C_3O_2 absorbs a single 193 nm photon and dissociates to yield C or C_2O [7, 21]. Processes (3) and (4) are the collision-induced mechanism for the C_2 high pressure band formation proposed by Kunz *et al.* [22]. Since the rate of diffusion at relatively high pressures above 1.0 Torr is expected to be quite slow (probably of the order of milliseconds), we believe that diffusion out of the observation space is negligible. Reactions (5) and (6) are the processes in which C and C_2O are removed. Under conditions such that the amount of C_3O_2 is sufficiently large compared with the amount of photolysis products, the reaction with C_3O_2 predominates over that with the photolysis products. Thus the concentration of C and C_2O can be described by the exponential functions

$$[C](t) = [C]_{t=0} \exp(-k_5 t) \quad (7)$$

$$[C_2O](t) = [C_2O]_{t=0} \exp(-k_6 t) \quad (8)$$

In accordance with processes (3) and (4) the rate equation for the $C_2^*(d\ ^3\Pi_g)$ concentration can be written as follows:

$$\frac{d[C_2^*]}{dt} = k_3[C][C_2O] - k_4[C_2^*] \quad (9)$$

An analytical solution of the differential equation (9) can be determined by substituting eqns. (7) and (8) into eqn. (9) and integrating over time with the Laplace transformation. It is

$$[C_2^*](t) = k_3[C]_{t=0}[C_2O]_{t=0}[\exp(-k_4 t) - \exp\{-(k_5 + k_6)t\}] \quad (10)$$

We shall analyse the dynamics of the C_2^* fluorescence using a model based on eqn. (10).

The equation predicts that the decay of C_2^* fluorescence can be described by a double-exponential function. Values of k_4 and $k_5 + k_6$ were derived from computer simulation to fit the observed data. Figure 7 presents examples of fluorescence data and fitted curves. The values of 220 and 270 ns for k_4^{-1} are in fair agreement with the values (200 ± 50 ns [19] and 170 ± 20 ns [20]) obtained from the direct measurement of the decay of the $C_2^*(d\ ^3\Pi_g)$ state. The tail of the fluorescence trace can be ascribed to processes involving the rate constants k_5 and k_6. The rate constant of the reaction $C + C_3O_2 \rightarrow$ products has been measured by Husain and Young [23]. Their values for k_5^{-1} (above 100 μs) are not compatible with our observed value. Therefore we attribute the slow component to process (6): $C_2O + C_3O_2 \rightarrow$ products. Unfortunately, we cannot detect this process directly by means of an appropriate procedure such as laser-induced fluorescence of C_2O. On the basis of the indirect evidence, however, we conclude that the slow component is a result of the reaction in which C_2O is removed by C_3O_2.

The emission intensity of the C_2 Swan band depends upon the square of the ArF laser power as shown in Fig. 3. This quadratic dependence can be explained on the assumption that single-photon absorption leads to the dissociation of C_3O_2 and produces a large amount of C and C_2O (eqns. (1) and (2)). According to eqn. (10) the concentration of C_2^* is proportional to the concentration of $[C]_{t=0}$ and $[C_2O]_{t=0}$. The secondary reaction mechanism for the production of $C_2(d\ ^3\Pi_g)$ explains well the initial intensity increment of the C_2 fluorescence seen in Fig. 2.

Acknowledgment

We are indebted to Dr. D. V. O'Connor for critical reading of the manuscript.

References

1 R. J. Donovan, in P. G. Ashmore and R. J. Donovan (eds.), *Gas Kinetics and Energy Transfer, Specialist Periodical Reports*, Vol. 4, Royal Society of Chemistry, London, 1981, p. 117.
2 E. B. Jenkins, D. C. Morton and A. V. Sweigart, *Astrophys. J., 157* (1969) 913.
3 W. T. Plummer and R. K. Carson, *Science, 166* (1969) 1141.
4 S. V. Filseth, *Adv. Photochem., 10* (1977) 1.
5 H. W. Thompson and N. Healey, *Proc. R. Soc. London, Ser. A, 157* (1936) 331.
6 K. Bayes, *J. Am. Chem. Soc., 83* (1961) 3712.
7 W. Braun, A. M. Bass, D. D. Davis and J. D. Simmons, *Proc. R. Soc. London, Ser. A, 312* (1969) 417.
8 N. Nishi, H. Shinohara and I. Hanazaki, *Chem. Phys. Lett., 73* (1980) 473.
9 D. A. Long, F. S. Murfin and R. L. Williams, *Proc. R. Soc. London, Ser. A, 223* (1954) 251.
10 R. W. B. Pearse and A. G. Gaydon, *The Identification of Molecular Spectra*, Wiley, New York, 1976.
11 K. P. Huber and G. Herzberg, *Constants of Diatomic Molecules*, Van Nostrand, New York, 1979.
12 J. E. Hesser, *J. Chem. Phys., 48* (1968) 2518.
13 J. G. Chervenak and R. A. Anderson, *J. Opt. Soc. Am., 61* (1971) 952.
14 G. Herzberg, *Molecular Spectra and Molecular Structure*, Vol. 1, *Spectra of Diatomic Molecules*, Van Nostrand, New York, 1950, p. 208.
15 Y. Osamura, K. Nishimoto, S. Yamabe and T. Minato, *Theor. Chim. Acta, 52* (1979) 257.
16 D. R. Stull and H. Prophet (eds.), *JANAF Thermochemical Tables, NBS Ref. Data Ser. 37*, 2nd edn., 1971 (National Bureau of Standards, U.S. Department of Commerce).
17 J. Bokor, J. Zavelovich and C. K. Rhodes, *J. Chem. Phys., 72* (1980) 965.
18 R. K. Dhumwad and N. A. Narasimhan, *Can. J. Phys., 46* (1968) 1254.
19 E. H. Fink and K. H. Welge, *J. Chem. Phys., 46* (1967) 4315.
20 W. H. Smith, *Astrophys. J., 156* (1969) 791.
21 V. M. Donnelly, W. M. Pitts and J. R. McDonald, *Chem. Phys., 49* (1980) 289.
22 C. Kunz, P. Harteck and S. Dondes, *J. Chem. Phys., 46* (1967) 4157.
23 D. Husain and A. N. Young, *J. Chem. Soc., Faraday Trans. II, 71* (1975) 525.